Photochemistry in Small Domains and Single Polymer Nanoparticles

*Satoshi Takahashi, Shinjiro Machida, and Kazuyuki Horie**

Department of Chemistry and Biotechnology, Graduate School of Engineering, University of Tokyo, 7-3-1 Hongo, Bunkyo-ku, Tokyo 113-8656, JAPAN

SUMMARY: In this article, our recent results of the application of near-field scanning optical microscopy (NSOM) to the photochemistry in small domains and single polymer nanoparticles are presented. After an introduction and the description of our apparatus, results on three topics are presented: (1) Control and observation of a photoacid generation from p-nitrobenzyl 9,10-dimethoxyanthracene-2-sulfonate (NAS) in a polymer thin film, (2) Patterning due to refractive index changes by a photoisomerization of 3-phenyl-2,5-norbornadiene-2-carboxylic acid (PNCA) (3) NSOM observation of moving nanoparticles at a liquid/solid interface.

Introduction

Studies of nano-organized supramolecular and macromolecular systems have been accelerated by recent developments in both synthetic techniques and characterization methods including spectroscopies and the family of scanning probe microscopies.

Optical techniques have been powerful tools to characterize and evaluate various optical properties, including absorption, fluorescence, refractive index, birefringence, and nonlinear susceptibilities of polymer materials. However, due to the diffraction limit of light[1] the spatial resolution of conventional microscopes is limited approximately to the half of the wavelength, usually 200 - 300 nm in visible region.

Near-field scanning optical microscopy (NSOM) is one of the optical methods to circumvent this diffraction limit[2]. In NSOM, instead of focusing light from a light source onto the sample, the light source, which is referred to as a probe, is placed in close proximity to the surface, and by raster-scanning the sample surface with the probe, the optical response from the sample is collected one pixel by another. The spatial resolution of NSOM is determined by the size of the light source and the distance between the probe and the sample, independent of the wavelength of the incident light. Theoretically atomic scale resolution may be possible.

 CCC 1022-1360/00/$ 17.50+.50/0

NSOM has therefore been investigated extensively for the past ten years[3] as a fascinating technique in order to observe the details of sample surfaces on the molecular-size scale.

We have demonstrated various kinds of NSOM including white light source imaging[4,5] and Raman spectroscopy[6], and applied NSOM to the investigation of photochemistry in small domains of polymer thin films[7-9]. The light from the NSOM probe has been used not only to produce photochemical products, but also to monitor their amount and diffusivity. However, care must be taken in order not to damage the photochemical products or the sample by the monitoring light. It is thus necessary to select a wavelength (in other words photon energy) of the monitoring light which should be nonresonant to the sample. It seems controversial because in such case no absorption or no fluorescence, i.e. no optical contrast is observed. In order to solve this problem, we employed two kinds of contrast mechanisms. One is the contrast of an indicator which couples with the photochemical products[7-8]. The indicator is selected so that it is resonant to the monitoring light, but nonresonant to the photoreaction light. The amount and spatial extension of the photochemical products will be mapped via those of the indicator. Another contrast mechanism is the changes in refractive index[9]. It is more complicated than the first one, and is more closely related to the physical basis of near-field optics. It is known that in near-field optics, the contrast is related to the conversion efficiency of the evanescent field localized to the probe aperture with the propagating light. It is analogous to the relation between the Rayleigh-scattering intensity and the dielectric constant of the scatterer in the far-field optics. Therefore the transmission of the sample increases with the increase in refractive index.

In this article, our recent results are presented. Following the description of our home-build NSOM apparatus, the results concerning three topics are presented: (1) Control and observation of a photoacid generation(2) Patterning due to refractive index differences, and (3) NSOM observation of moving nanoparticles at a liquid/solid interface.

NSOM apparatus

In most commonly used NSOM, optical fibers are used to fabricate small light source[10]. One

end of the optical fiber is tapered and metal-coated, with a very small aperture at the end of the taper. The diameter of the taper end is typically a few hundred nanometers and the aperture size is smaller than a hundred nanometers. By introducing laser light from the other fiber end and put the apertured end in proximity to the sample surface, the light emerging from the aperture illuminates a small area, as small as the aperture size, of the surface. The fluorescence and/or transmitted light is collected via a microscopic objective by a photodetector. To place the aperture in close to the sample surface a so-called shear force technique[11-12] is used. The fiber probe is dithered with a small piezo. When the probe contacts the sample surface, dither amplitude sharply decreases. Thus by monitoring the dither amplitude as a feedback signal, the distance between the probe and the surface is kept at a constant value.

The NSOM used in the present study was built in our laboratory, which is schematically illustrated in Fig. 1. NSOM probes were fabricated by a chemical etching method followed by aluminum coating on the sidewalls[13]. The sample is mounted on the sample stage connected with a piezo scanner to scan the sample. For shear force distance regulation, the NSOM probe was attached to a small piezoelectric transducer which vibrates the probe. The vibration amplitude of the probe is detected using an optical detection technique; a semiconductor laser (wavelength 670 nm) was focused onto the side of the NSOM probe and scattered light is collected by a photodiode which generates a feedback signal.

In order to examine the spatial resolution of our NSOM, a chromium test pattern was measured, as shown in Figure 2. This pattern has a period of 1 μm, and the chromium thickness is approximately 5 nm. The light source was a He-Cd laser with a wavelength of 442 nm. The bright squares in the topographic image are areas coated with chromium at which light is blocked, and the dark squares are bare glass substrate through which visible light can pass. The contrast of the NSOM image is inverted compared to the topographic image due to the opacity of the chromium film. The cross-section of the NSOM image along the line AB is also presented in Figure 2. Stronger NSOM signal is observed at the area of the bare glass, and the spatial resolution of the NSOM is estimated from the sharpness of the start (or end) of the signal increase (or decrease) at the edges of the square. The sharpness was defined as the width corresponding to the signal change from 10 % to 90 % of intensity maximum. Based

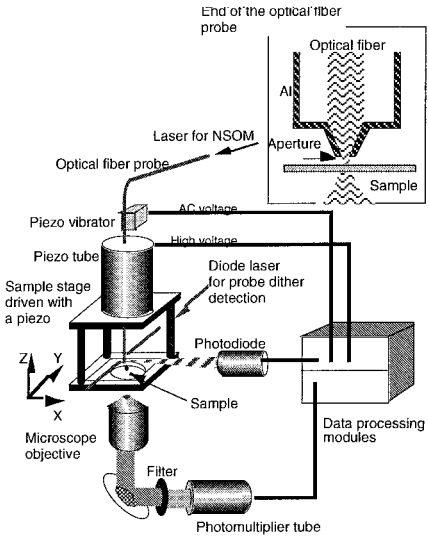

Fig. 1: Schematic illustration of our NSOM apparatus.

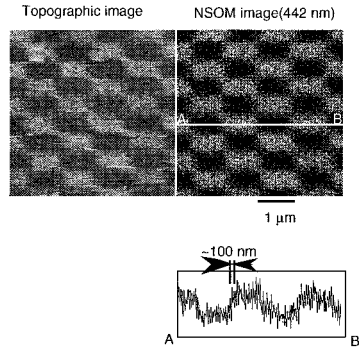

Fig. 2: Simultaneously obtained topographic image (left-hand side) and corresponding NSOM image (right-hand side) of a chromium test pattern. Bright regions in the topographic image correspond to deposited chromium with an average thickness of 5 nm. A cross-section along line AB in the NSOM image is also presented.

on this definition, the spatial resolution of our NSOM system is evaluated to be about 100 nm, twice as high as the diffraction limit.

Photoacid generation induced and monitored with NSOM

Photoacid generation and its diffusion in polymer films play important roles in the chemical-amplification-based photoresists in deep-UV lithography[14-15]. We have reported a spectroscopic method to evaluate the diffusion coefficient of a photoacid in a polymer solid[16], where the diffusion of the photoacid was analyzed using photoabsorption of a pH sensitive dye, Nile Blue A (NBA), doped together with the photoacid generator. In this section NSOM is implemented with this spectroscopic method[7-8] in order to induce and observe photoacid generation in a polymer solid film.

As a photoacid generator (PAG), p-nitrobenzyl 9,10-dimethoxyanthracene-2-sulfonate (NAS, **1**) was used [17]. The photoacid from NAS was monitored by the fluorescence from a pH sensitive dye, Nile blue A (NBA). The basic form of NBA **2** is so reactive with acidic

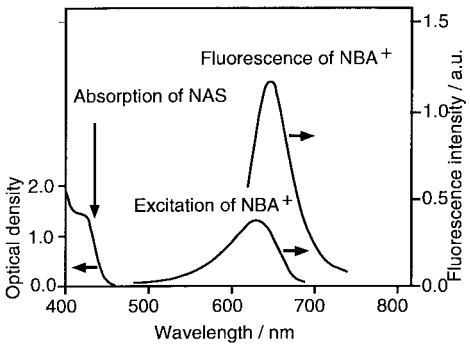

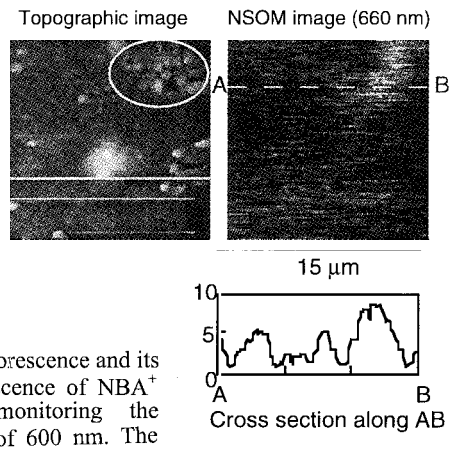

Fig. 3: An absorption spectrum of NAS, and fluorescence and its excitation spectra of NBA cation. The fluorescence of NBA^+ excitation spectrum was obtained by monitoring the was observed with an excitation wavelength of 600 nm. The fluorescence at 700 nm.

Fig. 4: (right): Simultaneously obtained topographic image (left-hand side) and corresponding fluorescent NSOM image (right-hand side) of a PMMA film doped with NAS and NBA. The film was exposed to 442 nm laser light from NSOM probe for 1 hour before obtaining the image. The excitation source was a DCM dye laser at 620 nm, and fluorescence from NBA cations at 660 nm is mapped with NSOM. A cross-section along line AB in the NSOM image is also displayed.

substances that its protonation proceeds irreversibly resulting in NBA cation **3** except under basic condition[18]. NBA base, NAS, and NaOH was added in a chloroform solution of Poly(methyl methacrylate) (PMMA) with a molar ratio of 1:2:1. and the obtained solution was cast onto a glass cover slip. An absorption spectrum of NAS, and fluorescence and its

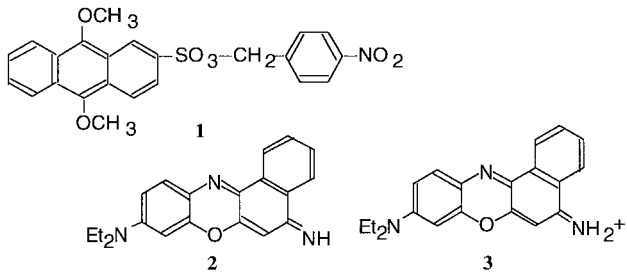

excitation spectra of NBA cation are displayed in Figure 3. From this figure it is observed that NAS has no absorption at 620 nm while NBA cation has a significant absorption there, indicating that the dye laser at 620 nm does not induce photoacid generation from NAS.

In Fig. 4 a fluorescence NSOM image of a NAS- and NBA- doped PMMA film after

photoacid generation is displayed. Photoacid generation was performed by positioning the NSOM probe at one point on the sample for about 1 hour, at which the sample is illuminated by the light (λ=442 nm) coming out from the aperture of the NSOM probe. The topographic image of the same area was obtained simultaneously. The circle shown in the upper right part in the topographic image indicates the area where the sample was irradiated with a 442 nm laser. In the corresponding area in the NSOM image, fluorescence signal originating from NBA cations is larger than in the other part, typically twice as large as other intensity maxima in the NSOM image. It can thus be concluded that the upper right area is acidified after the irradiation of 442 nm light.

Patterning of refractive index contrast

Fabrication and characterization of nanometer-scale patterns of refractive index are an important research subject from two standpoints: understanding the mechanisms of NSOM contrasts of dielectric materials and application to a high density optoelectronic integrated circuits. In this section, submircometer scale patterning of refractive index on a transparent polymer film is demonstrated for the first time by using NSOM.

The material used in this study is 3-phenyl-2,5-norbornadiene-2-carboxylic acid (PNCA **4**)[19] doped in poly(methyl methacrylate) (PMMA). The doping ratio of PNCA in the sample was 35 wt%. In our previous study this material was shown to perform a large refractive index decrease by UV light irradiation due to the photoisomerization of PNCA to 3-phenyl-quadricyclane-2-carboxylic acid (PQCA, **5**) [20]. The refractive index was measured with a

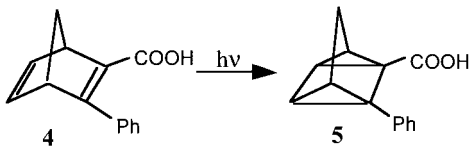

4 **5**

m-line method[21] before and after the 325 nm UV irradiation, yielding refractive index change (at 633 nm) from 1.540 to 1.534. Absorption spectra of PMMA-PNCA film (about 30 μm thick) during 325 nm UV irradiation is displayed in Fig. 5. It should be noted that PNCA-doped

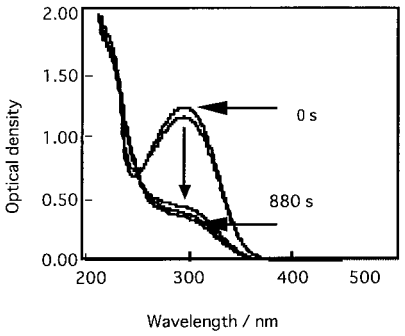

Fig. 5: Absorption spectra of PMMA-PNCA thin film during UV irradiation. The thickness of the film was 30 μm.

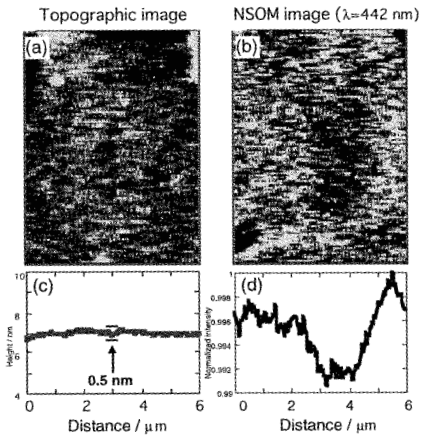

Fig. 6 (right): Topographic image (a) and corresponding transmission NSOM image (b) for UV-irradiated PMMA-PNCA thin film (3 μm thick). The wavelength for obtaining the NSOM image was 442 nm. The irradiated area was a vertical line with a length of 4 μm located at the center of the image. The averaged cross sections for (a) and (b) are displayed in (c) and (d), respectively. The averaging was performed for all the horizontal lines which contain the irradiated area.

PMMA is transparent for visible light both before and after photoisomerization.

The irradiation of UV light was performed by coupling He-Cd laser light (325 nm) to an optical fiber probe scanning over the sample surface. For patterning the NSOM probe coupled with the UV light scanned a single line with a length of 4 μm. After the irradiation, transmission NSOM image was obtained at an incident wavelength of 442 nm.

In Fig. 6, simultaneously obtained topographic image and corresponding NSOM image (taken at 442 nm) are presented. The UV-irradiated line is located vertically at the center of the image. The topographic change is almost negligible. In contrast to the topographic image, there is a dark band in the NSOM image observed around the irradiated region. In order to evaluate the topographic and near-field optical contrasts more precisely, the averaged cross sections of the images are produced. Figs. 6c and 6d are the cross sections of 128 horizontal lines containing the irradiated area in Figs. 6a and 6b, respectively. The topographic change is about 0.5 nm (Fig. 6c) which is smaller than those reported in other photochemical

modifications (typically larger than 10 nm) and is almost negligible for characterizing the optical properties of the thin film sample. The cross section of the NSOM image normalized with the maximum value (Fig. 6d) shows a clear contrast created by the UV irradiation. The relative optical contrast is about 0.5 %. The width of the band observed in Fig. 6d is somewhat broadened, considering that the NSOM probe scanned a single line. However the sharpness of the edges of the pattern is more favorable (about 300 nm) compared to the width of the band (about 2 μm). Because the edge sharpness is also broadened in the far-field illumination, it can be concluded from Fig. 6d that the image acquisition is performed in near-field regime, but only the aperture diameter itself was not small enough in the present experiment.

Polymer nanoparticles moving at a liquid/solid interface

In this section, we propose the use of NSOM as a novel method to detect analytes moving along the liquid/solid interfaces of microchannels of fluid.

We have developed a fluid cell with an aqueous channel (3 mm wide, 25 mm long, and 150 μm deep) so that the mechanical damping of the probe vibration during shear force detection is reduced. The channel was filled with a phosphoric acid buffer solution, and NSOM observation was performed at the liquid/solid interface in the channel. Dye-doped latex beads with a diameter of 500 nm were added in the buffer layer, and NSOM fluorescence images of the beads placed at the liquid/glass interface of the fluid cell have been obtained. A topographic image and corresponding NSOM fluorescence image is shown in Fig. 7. The excitation and fluorescence wavelengths are 442 nm and 550 nm, respectively. In spite of the absence of any features in the corresponding topographic image, a few spots originating from the fluorescent beads are observed, with one of them clearly visible. The average diameter of the spots observed in Fig. 7 is about 2 μm, four times larger than the nominal diameter of the beads. A possible reason is that the bead is loosely bound to the liquid/sold interface and is fluctuating by Brownian motion. This is supported by the absence of the corresponding topographic image which is less sensitive to the fragile surface.

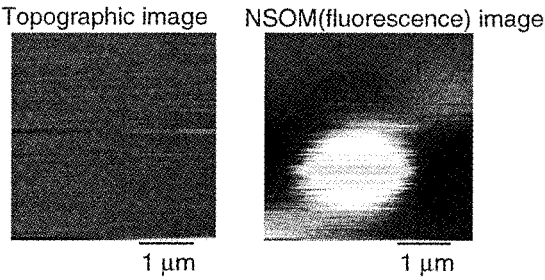

Fig.7: Topographic image (left) and corresponding NSOM fluorescence image (right) of 500 nm polystyrene beads placed at the liquid/glass interface of the home-built fluid cell.

Summary

In this article, our recent results concerning the application of near-field scanning optical microscopy (NSOM) to the photochemistry in small domains and single polymer nanoparticles are presented. Photoacid generation from NAS in a polymer thin film is induced and mapped by using a pH indicator, NBA. Refractive index contrast is formed in a PNCA-doped polymer film, and is observed by transmission NSOM. Finally, NSOM observation of single latex spheres placed at a liquid/solid interface is demonstrated, implying a potential application of NSOM to a high resolution detector in micro fluid networks and miniaturized electrophoresis instruments.

References

1. M. Born, E. Wolf, *Principles of Optics,* 6th ed., Cambridge University Press, Cambridge 1980.
2. D. W. Pohl, in *Near Field Optics* (NATO ASI Ser. E, vol. 242), D. W. Pohl, D. Courjon (Eds.), Kluwer Academic Pub., Dordrecht 1993, p. 1, and references there in.
3. R. C. Dunn, *Chem. Rev.* **99** 2891 (1999).
4. S. Takahashi, T. Fujimoto, K. Kato, I. Kojima, *Nanotechnol.* **8**, A54 (1997).
5. S. Takahashi, M. Futamata, I. Kojima, *Bunseki-Kagaku* **47**, 1055 (1998) (in Japanese).
6. S. Takahashi, M. Futamata, I. Kojima, *J. Microscopy* **194**, 519 (1999).
7. M. Machida, M. Shigyo, A. Yamakawa, H. Osawa, K. Horie, *Tech. Dig. 5th International Conference on Near Field Optics and Related Techniques*, Shirahama, **1998**, 297.
8. S. Takahashi, S. Machida, K. Horie, *J. Photopolym. Sci. & Technol.* **13**, 231 (2000).
9. S. Takahashi, K. Samata, H. Muta, S. Machida, K. Horie, *Appl. Phys. Lett.*, submitted.
10. E. Betzig, J. K. Trautman, *Science* **257**, 189 (1992).

11. E. Betzig, P. L., Finn, J. S. Weiner, *Appl. Phys. Lett.* **60**, 2484 (1992).
12. Toledo-Crow, R.; Yang, P. C.; Chen, Y.; Vaez-Iravani, M. *Appl. Phys. Lett.* **1992**, *60*, 2957.
13. Ohtsu, M. Ed. Near-Field Nano/Atom Optics and Technology, Springer-Verlag Tokyo, 1998.
14. Ito H. *IBM J. Res. Develop.*, **1997**, *41*, 69.
15. MacDonald, A; Willson, C. G.; Frechet, M. J. *Acc. Chem. Res.*, **1994**, *27*, 151.
16. A. Yamakawa, K. Horie, *J. Photopolym. Sci & Technol.*, **12**, 297 (1999).
17. T. Omote, K. Koseki, T. Yamaoka, *Macromolecules* **23**, 4788 (1990).
18. M. M. Davis, H. B. Hetzer, *Anal. Chem.* **38**, 451 (1966).
19. I. Nishimura, A. Kameyama, T. Sakurai, K. Nishikubo, *Macromolecules* **29**, 3818 (1996).
20. K. Kinoshita, K. Horie, S. Morino, T. Nishikubo, *Appl. Phys. Lett.* **70**, 2940 (1997).
21. S. Morino, S. Machida, T. Yamashita, K. Horie, *J. Phys. Chem.* **99**, 12080 (1995).